Multi-stack Technique for a Compact and Wideband EBG Structure in High-Speed Multilayer Printed Circuit Boards

Myunghoi Kim

We propose a novel multi-stack (MS) technique for a compact and wideband electromagnetic bandgap (EBG) structure in high-speed multilayer printed circuit boards. The proposed MS technique efficiently converts planar EBG arrays into a vertical structure, thus substantially miniaturizing the EBG area and reducing the distance between the noise source and the victim. A dispersion method is presented to examine the effects of the MS technique on the stopband characteristics. Enhanced features of the proposed MS-EBG structure were experimentally verified using test vehicles. It was experimentally demonstrated that the proposed MS-EBG structure efficiently suppresses the power/ground noise over a wideband frequency range with a shorter port-to-port spacing than the unit-cell length, thus overcoming a limitation of previous EBG structures.

Keywords: Electromagnetic bandgap (EBG), Miniaturization, Multi-stack (MS), Noise suppression, Printed circuit boards, Vertical branch.

I. Introduction

Signficant attention has recently been focused on the design of high-speed multilayer printed circuit boards (PCBs). Because numerous mixed-signal devices are integrated into a limited area of PCBs and commonly share metal traces and planes, the use of multiple layers in high-speed PCBs is in high demand. By employing many layers, the device layout and placement have become more convenient, whereas the signal and power integrity issues have become more complex.

Among these issues, noise coupling through power and ground planes in multilayer PCBs is a major concern for high-performance mixed-signal systems. In recent high-speed PCBs, various devices (for example, high-speed microprocessors, RF circuits, analog devices, and optical sensors) are integrated into a single board, and placed within a small area, thus reducing the device-to-device spacing. To deliver power to these circuits, metal planes are commonly used and shared by various devices. The multiple metal planes are parallel plate waveguides and cavity resonators in view of electromagnetic wave propagation. The parallel plate waveguide and cavity resonator excite numerous resonance peaks resulting in serious noise couplings [1], [2]. Furthermore, continuous increases in the clock frequency and data rates for high-speed digital systems significantly widen the spectra of power/ground noise so that it spans a frequency range of several GHz. The wideband power/ground noise severely deteriorates the system performance by reducing the noise margin and degrading the RF sensitivity [3]–[5]. Therefore, it is imperative to suppress the power/ground noise over a wideband frequency range in

Manuscript received Nov. 19, 2015; revised May 7, 2016; accepted May 16, 2016.

Myunghoi Kim (mhkim80@hknu.ac.kr) is with the Department of Electric, Electronic and Control Engineering, Hankyong National University, Anseong, Rep. of Korea.

multilayer high-speed PCBs.

Electromagnetic bandgap (EBG) structures have been introduced to achieve wideband suppression of power/ground noise in multilayer PCBs [6]–[13]. One of the main topologies of EBG structures is based on a periodic impedance perturbation using stepped impedance (SI) structures [9]–[13]. A number of studies have been conducted on SI-EBG structures owing to their simple design, wideband stopband, high suppression level, and easy board integration. In particular, the VSI-EBG structure [13] substantially improves the noise suppression performance by employing multiple variations of characteristic impedances along the EBG patches. However, it still requires a large board area. Hence, previous EBG structures have drawbacks for high-speed PCBs where mixed-signal devices are densely packed. First, this structure requires a large space on a board to ensure the periodicity of the EBG cells. Moreover, the lateral distance between the noise source and the victim device needs to be quite long to obtain the high level and wideband bandwidth of noise suppression. In addition, the performances of the EBG structures may be easily influenced and degraded by other planes above or below the EBG layer. In other words, many design constraints should be considered to avoid degrading the noise suppression of the EBG structures.

To overcome these drawbacks, partial placement techniques were introduced in [14] through [17]. These approaches reduce the EBG area compared to an EBG structure that is fully occupied on a board. However, the lateral distance from the noise source to the victim device needs to be longer than a unit-cell (UC). Additionally, non-periodicity, induced by an insufficient number of EBG cells, results in the degradation of the suppression level and the stopband bandwidth compared to a fully arranged EBG structure. Therefore, we need a new EBG structure to achieve wideband and high noise suppression within a shorter distance than a UC length.

In this paper, we propose a multi-stacked EBG (MS-EBG) structure dedicated to multilayer PCBs to reduce the lateral area, wideband noise suppression, and a short distance between the noise source and victim devices. An analytical equation for the dispersion characteristics of the proposed MS-EBG structure is extracted. Based on this equation, the effects of a multi-stack technique on the dispersion characteristics are examined. The advantageous features of the MS-EBG structure are experimentally verified through various test vehicles.

II. Multi-stacked EBG (MS-EBG) Structure

The proposed MS-EBG structure consists of capacitive patches and inductive branches to induce stepped impedance resonators, as shown in Fig. 1. A rectangular patch and corresponding ground planes form a low characteristic impedance (low-Z) part, whereas small rectangular patches and a vertical via structure form a high-Z part. The low-Z parts are distributed vertically in multilayer PCBs. The low-Z parts in different layers are connected to each other through inter-/intra-cell branches comprising small rectangular patches and a via structure. Note that adjacent low-Z parts on the same layer are

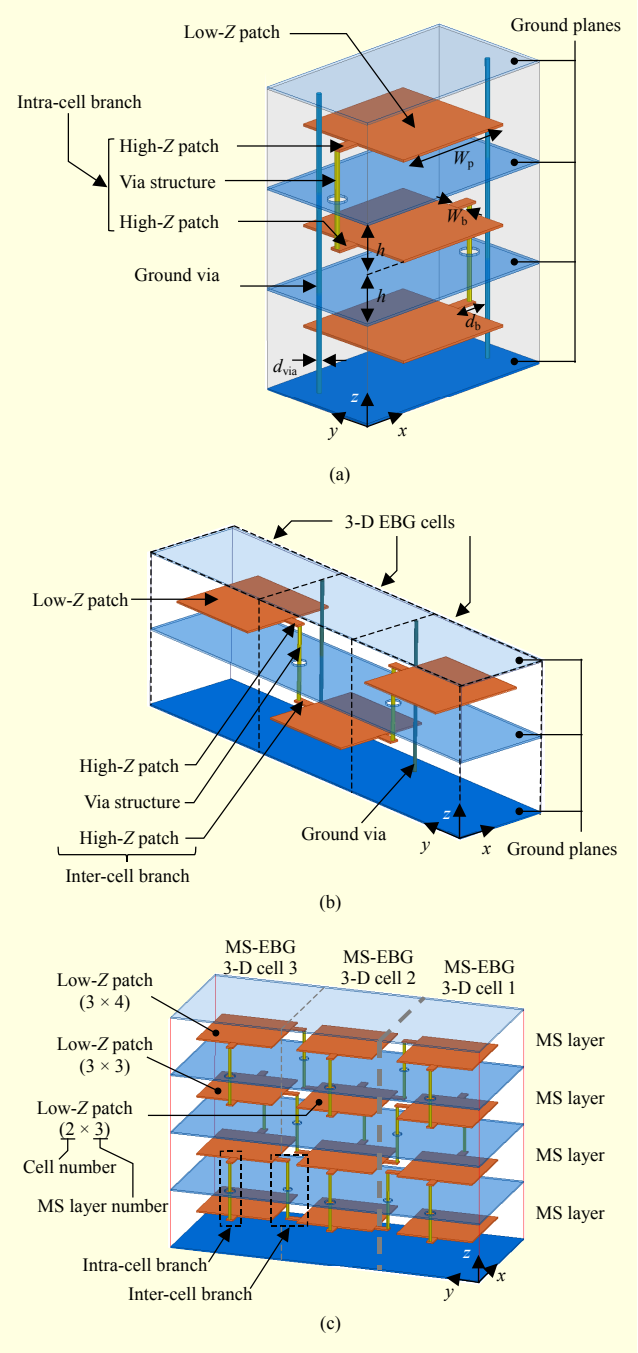

Fig. 1. (a) 3-D cell of proposed multi-stacked EBG (MS-EBG) structure with intra-cell branches, (b) 3-D EBG cells with inter-cell branches, and (c) 3 × 4 MS-EBG structure.

ETRI Journal, Volume 38, Number 5, October 2016
http://dx.doi.org/10.4218/etrij.16.0115.0997

not connected. Ground planes are connected with each other using ground via structures. Note that, for the sake of simplicity, a ground via is not shown in Fig. 1(c). Vertical branches are employed at every side of the rectangular patch for connection with low-Z parts in different layers, thus achieving a two-dimensional (2-D) periodic arrangement of the EBG cells. Figure 1(a) illustrates a three-dimensional (3-D) EBG cell implemented by applying the MS technique. In the 3-D EBG cell, low-Z patches are connected with each other using intra-cell branches. Ground via structures are located near the intra-cell branches. In Fig. 2(b), three 3-D cells are shown with inter-cell branches. The low-Z patches in the different 3-D cells are connected through the intra-branches. Combining the intra- and inter-cell branches, the 3 × 4 MS-EBG structure is configured as shown in Fig. 1(c). The size of the MS-EBG structure can be defined by $M \times N$, where M and N represent the numbers 3-D cells and MS layers corresponding to the number of low-Z patches in a 3-D cell, respectively. The proposed MS technique uses vertical braches consistently to connect all EBG cells. Consequently, it ensures that the MS-EBG structure is a 2-D homogenous structure to achieve high suppression of the power/ground noise and wideband bandwidth of the stopband.

The lateral area of the MS-EBG structure in Fig. 1(c) is equal to that of a planar EBG structure with 1 × 3 EBG cells. The MS-EBG structure needs more layers to reduce the lateral area for the EBG structure. However, in many applications, increasing the number of layers is more beneficial and desirable than increasing the lateral area because the EBG structure, which occupies the entire PCB area, leads to design constraints and is influenced by other planes on the PCBs. In addition, the MS-EBG structure has the advantage of a substantial reduction in the distance between a source and victim, which will be proved throughout this paper.

III. Dispersion Analysis

The noise suppression principle for the MS-EBG structure can be explained using a stepped impedance resonator theory [9]. As shown in Fig. 2(a), a noise wave propagates through power/ground planes that have low and high characteristic impedances (low-Z and high-Z) in the proposed MS-EBG structure. An abrupt change in the characteristic impedance causes the phenomena of electromagnetic wave reflection and scattering. This periodic impedance change results in an electromagnetic bandgap where propagation of electromagnetic waves is prohibited. In addition, the vertical branch provides an inductive path, thus improving the stopband bandwidth.

To investigate the noise propagation characteristics, the proposed MS-EBG structure is modeled as an equivalent transmission line circuit. The low-Z part is modeled as the transmission lines with characteristic impedance Z_{oL} and length of W_p, whereas the high-Z part is modeled as the branch inductance (L_b) and via inductance (L_V), as shown in Fig. 2(a).

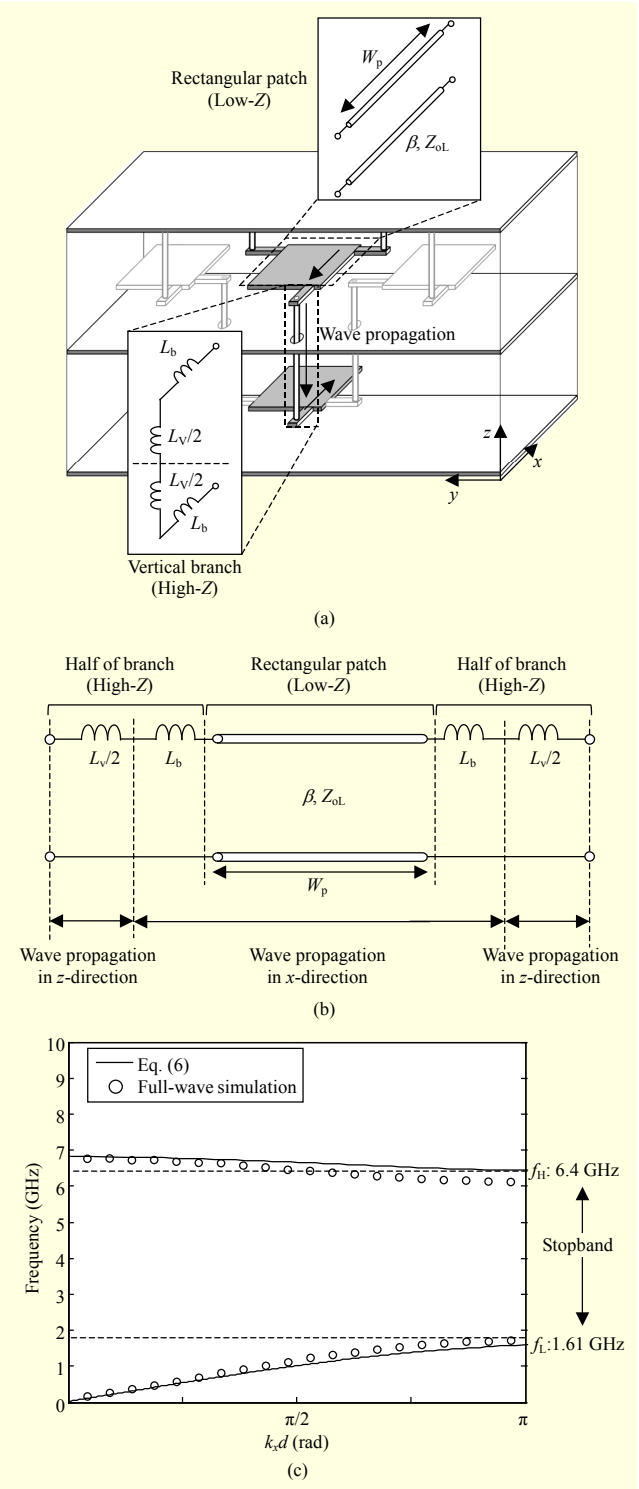

Fig. 2. (a) Model based on a transmission line, (b) equivalent circuit for dispersion analysis, and (c) dispersion diagram of MS-EBG structure.

For the sake of simplicity, the ground via structures are not shown in this figure. In the circuit model, the intra-/inter-cell branches are equivalently modeled as inductors with an approximate value. Note that the ground via inductance is assumed to be zero in the equivalent model for model simplicity. A full equivalent model of the EBG cell (that is, the low-Z part and vertical branches for an intra- or inter-cell branch) is obtained as shown in Fig. 2(b). In the full equivalent model of the EBG cell, L_{vb} is the sum of half the power via inductance $L_v/2$ and the branch inductance L_b. The values of L_v and L_b can be estimated as follows [18]:

$$L_v = \frac{\mu_o h}{\pi}\left[\ln\left(k+\sqrt{1+k^2}\right)-\sqrt{1+k^{-2}}+k^{-1}+0.25\right], \quad (1)$$

$$L_b = \mu_o h \frac{d_b}{2W_b}, \quad (2)$$

$$L_{vb} = \frac{L_v}{2+L_b}. \quad (3)$$

Here, μ_o is the permeability of a free space and $k = 4h/r_v$. h is the distance between the power and ground planes, where r_v is the radius of the via structure. The phase constant β is given by

$$\beta = \frac{2\pi f\sqrt{\varepsilon_r}}{c}, \quad (4)$$

where ε_o and ε_r are the permittivity of the free space and the relative dielectric constant, respectively, and c is the speed of light in a vacuum.

To predict the dispersive characteristics of the proposed MS-EBG structure, Floquet's theory is applied [19]. The propagation in the periodic EBG cells is analyzed using ABCD parameters where the unit cell has an effective phase constant k_x as follows:

$$\begin{pmatrix} A_{eff} & B_{eff} \\ C_{eff} & D_{eff} \end{pmatrix} = \begin{pmatrix} \cos(k_x d) & jZ_o \sin(k_x d) \\ jY_o \sin(k_x d) & \cos(k_x d) \end{pmatrix}$$

$$= \begin{pmatrix} 1 & Z_{vb} \\ 0 & 1 \end{pmatrix}\begin{pmatrix} \cos(\beta W_p) & jZ_{oL}\sin(\beta W_p) \\ jY_{oL}\sin(\beta W_p) & \cos(\beta W_p) \end{pmatrix}\begin{pmatrix} 1 & Z_{vb} \\ 0 & 1 \end{pmatrix}, \quad (5)$$

where $d = W_p + 2L_b$, $Z_{vb} = j\omega L_{vb}$, and $Y_p = 1/j\omega C_p$. From (5), the analytical dispersion equation for the proposed MS-EBG structure is given by

$$\cos(k_x d) = \cos\left(\beta W_p\right) - \frac{2\pi f L_{vb}}{Z_{oL}}\sin\left(\beta W_p\right). \quad (6)$$

We can find lower and higher cutoff frequencies (f_L, f_H) by setting $\mathrm{Re}\{k_x d\} = \pi$. The left-hand side of (6) is $\cos(k_x d) = -1$. The dispersion equation in (6) can then be expressed as

$$\left[\cos\left(\frac{\beta W_p}{2}\right) - \frac{2\pi f L_{vb}}{Z_{oL}}\cdot\sin\left(\frac{\beta W_p}{2}\right)\right]\cos\left(\frac{\beta W_p}{2}\right) = 0. \quad (7)$$

From (7), we can obtain the equations for f_L and f_H as follows.

$$\left[\cos\left(\frac{\beta W_p}{2}\right) - \frac{2\pi f L_{vb}}{Z_{oL}}\cdot\sin\left(\frac{\beta W_p}{2}\right)\right] = 0, \quad (8)$$

$$\cos\left(\frac{\beta W_p}{2}\right) = 0. \quad (9)$$

We can solve the equations explicitly for the cutoff frequencies. Note that a small angle approximation in (8) is assumed for f_L. The closed-form expressions for f_L and f_H are given by

$$f_L = \frac{1}{2\pi}\left(\frac{2Z_{oL}c}{L_{vb}W_p\sqrt{\varepsilon_r}}\right), \quad (10)$$

$$f_H = \frac{c}{2W_p\sqrt{\varepsilon_r}}. \quad (11)$$

From (10), a reduction in f_L can be achieved by decreasing the Z_{oL} value and increasing the inductances of intra-/inter-cell branches and low-Z patch size. From (11), f_H is increased by increasing W_p and is independent of Z_{oL} and L_{vb}.

The dispersion diagram of the MS-EBG structure is obtained using (6), as shown in Fig. 2(c). In the next section, an example structure for the dispersion analysis, as shown in Table 2, is used. In the dispersion analysis results, passbands and stopbands appear alternately. In this paper, we focus on the first stopband, which starts at the frequency of the first passband of $k_x d = \pi$ and ends at the frequency of the second passband of $k_x d = \pi$. These frequencies are called the lower cut-off frequency (f_L) and higher cut-off frequency (f_H). From the dispersion analysis, the stopband is formed in the wideband frequency range of 1.61 GHz to 6.4 GHz. The results from (6) agree well with those of the full-wave simulation using HFSS, as shown in Fig. 2(c). Hence, it is expected that the MS-EBG structure

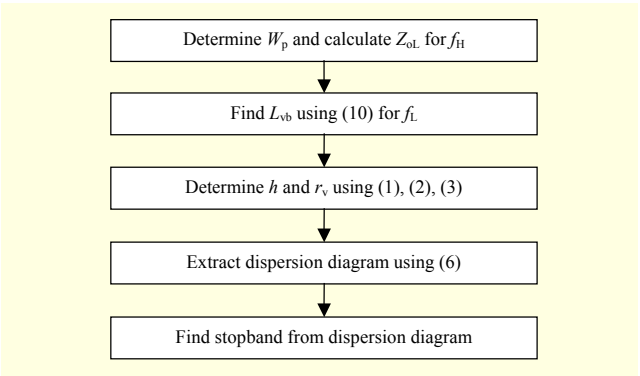

Fig. 3. Design procedure for proposed MS-EBG structure.

http://dx.doi.org/10.4218/etrij.16.0115.0997

Table 1. Summary of multi-stack technique effect on stopband characteristics with variations in via diameter.

d_{via} (mm)	L_{vb} (pH)	(10)	(11)	Full-wave simulation	
		f_L (GHz)	f_H (GHz)	f_L (GHz)	f_L (GHz)
0.2	225	1.65	6.1	1.46	6.4
0.3	193	1.69	6.1	1.58	6.4
0.4	177	1.72	6.1	1.65	6.4
0.5	167	1.74	6.1	1.70	6.4
0.6	160	1.76	6.1	1.73	6.4
0.7	155	1.77	6.1	1.76	6.4

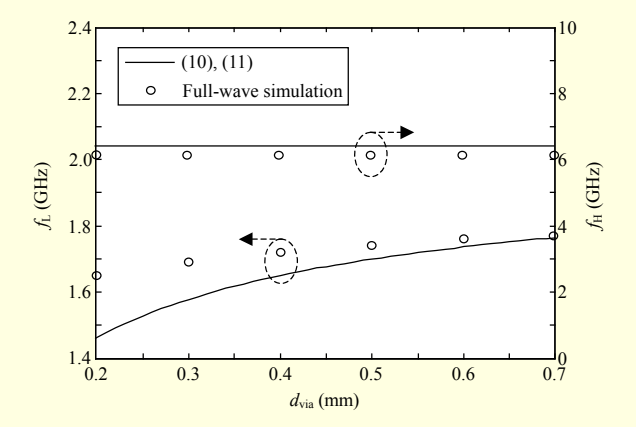

Fig. 4. Stopband characteristics (f_L, f_H) with various via diameter values.

significantly suppresses the power/ground noises over the broadband frequency range. For the proposed MS-EBG structure, the design procedure based on the above equations is shown in Fig. 3.

A primitive difference of the MS-EBG structure from previous planar EBG structures is the inductive characteristics of inter-/intra-cell branches. To further examine the inductive effect on a stopband, f_L and f_H values are obtained using (10), (11), and full-wave simulations for various via diameter values of d_{via} = 0.1 mm, 0.2 mm, 0.3 mm, 0.4 mm, 0.5 mm, 0.6 mm, and 0.7 mm. Note that the branch inductance decreases as the value of d_{via} ($2r_v$) increases. Figure 4 illustrates the cutoff frequencies obtained from (10) and (11), and the full-wave simulation with respect to the various d_{via} values. As can be seen in Fig. 4, the f_L values shift to lower frequencies as d_{via} decreases, whereas the f_H values are constant. As a consequence, the stopband bandwidth can be extended to a low frequency by increasing the inductance value of the intra-/inter-cell branches. Note that a reduced f_L value implies that the unit-cell size can be miniaturized for EBG structures based on a stepped impedance resonator [13]. Therefore, the proposed MS-EBG structure reduces the EBG array size as well as the unit-cell size compared to a non-stacked planar EBG structure. This effect of the multi-stack technique on the bandgap characteristics is summarized in Table 1.

IV. Experimental Results

To experimentally verify the proposed MS-EBG structure, test vehicles (TVs) were fabricated using a commercial PCB process with through-hole via structures. Four TVs (TV-1A, TV-1B, TV-1C, and TV-1D) were fabricated to demonstrate the proposed MS-EBG structure. TV-1A and TV-1C are power/ground planes without EBG structures as reference boards. The port location of TV-1A is the same as that of TV-1B, whereas TV-1C has the same port location as TV-1D. TV-1B and TV-1D are the proposed MS-EBG structures that use multi-stacks of 1 × 5 arrays. The difference between them is the port location. In TV-1B, the distance between the source port and the victim port is less than a unit-cell length, whereas the port-to-port spacing in TV-1D is approximately equal to five unit-cell lengths. The TVs will show that the MS-EBG structure suppresses the power/ground noise over a wideband frequency range in both a short source-to-victim distance (less than one unit-cell length) and relatively long distance (five unit-cell lengths). The scattering parameters are measured from 100 MHz to 10 GHz using an Agilent N5230A vector network analyzer and a Cascade GS-type 250-μm-pitch microprobe.

For the PCB process, FR-4 material is used as a dielectric substance. Its relative permittivity (ε_r) and loss tangent ($\tan\delta$) are 4.4 and 0.03, respectively. Copper is used in the conducting layers, the thickness of which is 18-μm thick. The MS-EBG structure is formed using 13 conducting layers. This value may be considered a huge value. However, various applications of high-speed PCBs for computer devices, networks, and server applications adopt a number of layers. The sizes of the low-Z patch and the high-Z branch are 11 mm × 11 mm and 1 mm × 2 mm, respectively. The length of the via structure is 0.2 mm. Its radius is 0.3 mm. The dimensions for the TVs of case 1 are summarized in Table 2.

Figure 5 depicts perspective views for TV-1B and TV-1D. For the sake of simplicity, ground via structures are not provided in Fig. 5(a). The proposed MS technique effectively

Table 2. Design parameters and TV dimensions.

Parameters	W_p	d_b	W_b	h	r_v
mm	11	2	1	0.1	0.3

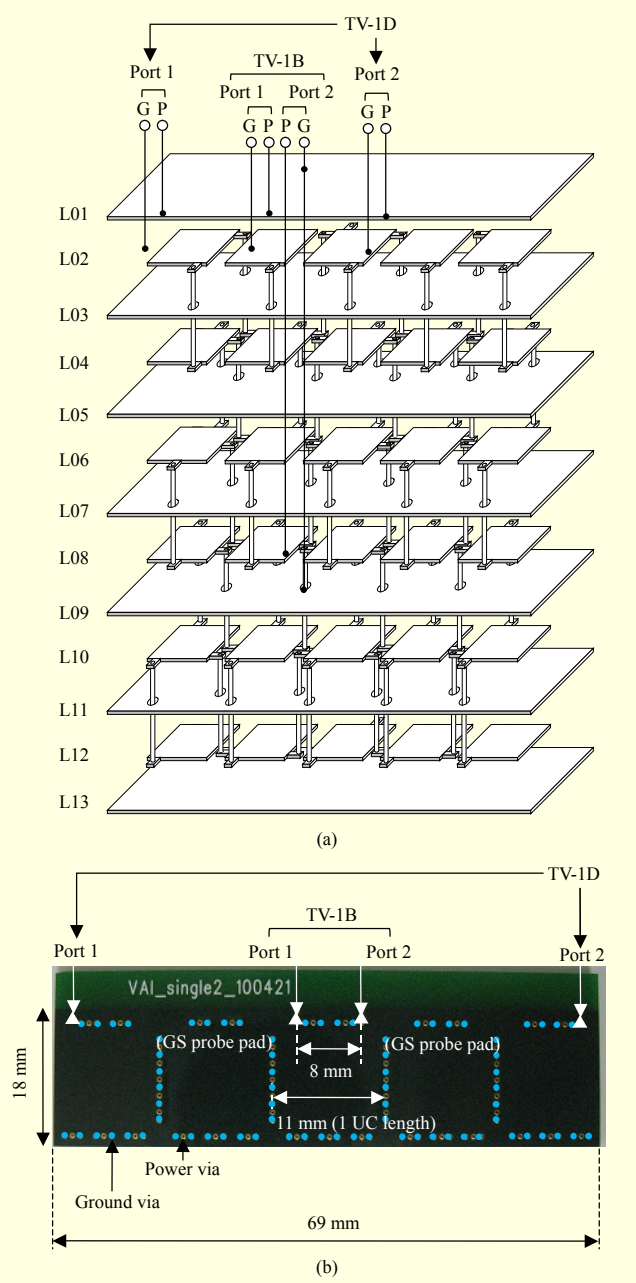

Fig. 5. (a) Illustrations of TV-1B and TV-1D and (b) photograph of TV-1B and TV-1D.

places 5 × 6 EBG arrays in a small area equal to the area occupied by 5 × 1 planar EBG arrays.

To measure the S-parameters of the TVs and minimize the parasitic effects, a GS-type microprobe is used. The port connection for the measurements is illustrated in Fig. 5(b). For the GS-type pads of port 1 in TV-1B, one pad is connected to the low-Z patch in the third cell and MS layer 6 through a via structure, and the other pad is connected to the ground planes through the ground via structures, which are omitted in Fig. 5(b). For port 2, one pad is connected to the low-Z patch in

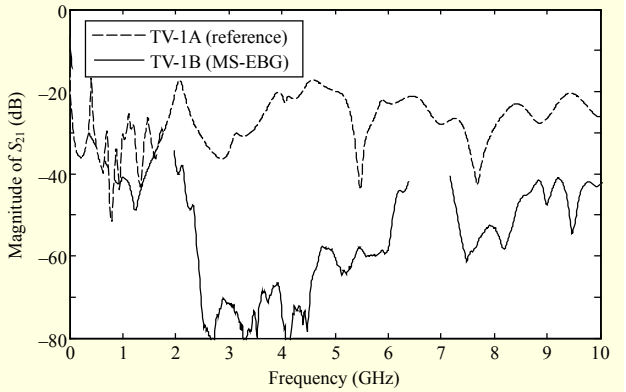

Fig. 6. Measured S_{21} results of TV-1A and TV-1B.

the third cell and MS layer 1, and the other pad is connected to the ground planes. Similarly, ports 1 and 2 in TV-1D are connected to the low-Z patches and ground planes, as shown in Fig. 5(a). TV-1D is designed to verify the wideband suppression between distant ports. Therefore, the ports are located at the edge cells (the first and last cells) and placed far away from each other. The distance is 64 mm, which is comparable to a five unit-cell length, whereas the lateral distance between the ports of TV-1B is 8 mm, which is less than the unit-cell length of 15 mm, as shown in Fig. 5(b).

The measured S_{21} results of TV-1A and TV-1B are shown in Fig. 6. The S_{21} curve of TV-1A shows numerous cavity resonances resulting in significant noise coupling. However, for TV-1B (MS-EBG), a wideband suppression with a –30 dB level is achieved within the frequency range of 2.1 GHz to 6.4 GHz. The results show a good correlation with the dispersion results of f_L = 1.61 GHz and f_H = 6.4 GHz. Remarkably, this wideband suppression with a high isolation level is accomplished with a port distance shorter than a unit-cell length. This implies that mixed-signal devices can be placed densely without a performance degradation caused by power/ground noise. For instance, in high-performance server and network applications, the MS-EBG structure is highly desirable and quite advantageous even if many layers are required.

In Fig. 7, the measured S_{21} results for TV-1C and TV-1D are depicted. TV-1D demonstrates the noise suppression between distant ports. The MS-EBG structure also suppresses the power/ground noise for ports placed far away from each other. Comparing the measurements of TV-1B, shown in Fig. 6, and TV-1D, shown in Fig. 7, a difference is observed at around 6.5 GHz. TV-1D seems to achieve more wideband suppression than TV-1B. The difference originates from the additional suppression of a second passband by increasing the number of EBG cells where noise is propagating. Consequently, the measurements demonstrate that the MS-EBG structure

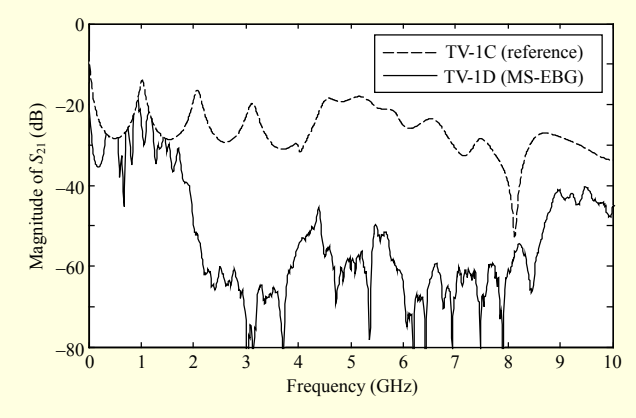

Fig. 7. Measured S_{21} results of TV-1C and TV-1D.

Table 3. Performance comparison of EBG structures.

EBG structure	f_L (GHz)	f_H (GHz)	Size (mm × mm)	Distance from source to victim (mm)
[9]	2.3	4.5	91.5 × 45.6	90
[11]	1.0	4.0	90 × 90	69
[13]	0.65	20	147 × 147	88
This work	2.1	6.4	18 × 69	8

effectively mitigates the power/ground noise for short and long distances between a noise source and victim. A performance comparison between the previous structures and the proposed MS-EBG structure is illustrated in Table 3. As shown in the table, the proposed structure has the advantages of a small size and short distance between a source and victim compared to the previous structures. Moreover, the MS-EBG structure has solid power/ground planes and thus the return path discontinuity is minimized and a good signal integrity performance can be expected.

Additionally, the proposed MS-EBG structure was compared with the previous stepped-impedance EBG (SI-EBG) structure. As shown in Fig. 8(a), the unit cell of the SI-EBG structure is designed to have the same dimensions as the MS-EBG structure. The array size of the SI-EBG structure is 5 cells × 6 cells. The ports are located in the center cell, as shown in Fig. 8(a). The distance between the ports is 8 mm, which is equal to that of the MS-EBG structure. The S_{21} results were obtained using electromagnetic simulations, as shown in Fig. 8(b). The S_{21} result of the MS-EBG structure shows a wideband suppression of the power/ground noise. In contrast, the SI-EBG structure does not effectively suppress the power/ground noise. The stopband for the power/ground noise is not clearly seen. Consequently, the MS-EBG structure substantially improves the noise suppression characteristics for

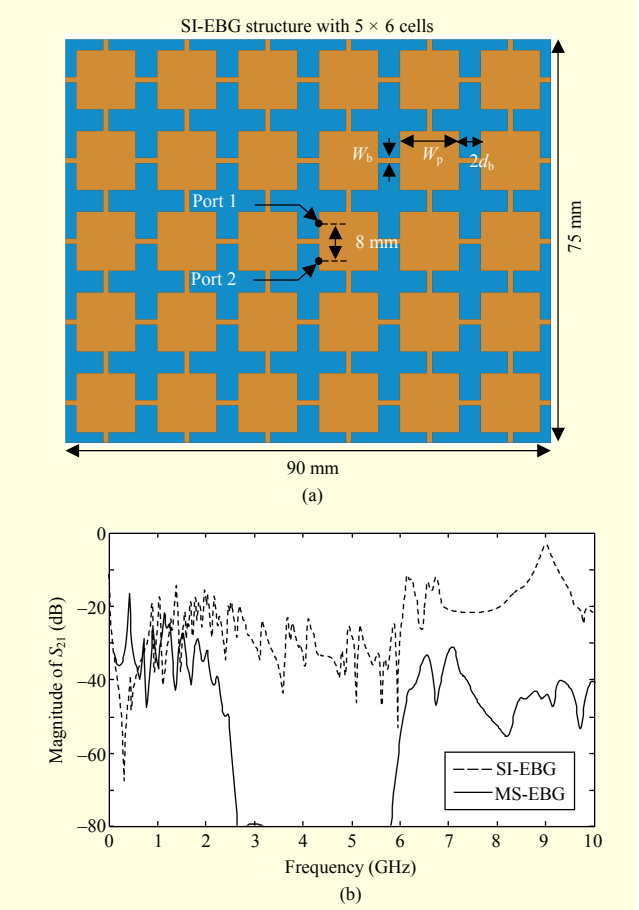

Fig. 8. (a) Previous stepped-impedance EBG (SI-EBG) structure with 5 cells × 6 cells and (b) simulated S_{21} results of a previous SI-EBG structure and the proposed MS-EBG structure.

the short distance between a source and victim ports.

V. Conclusion

A novel multi-stack technique for improving the EBG structures in high-speed multilayer PCBs was presented. To estimate the stopband characteristics, a dispersion equation was extracted, and shows a good correlation with the measurements. The proposed approach was experimentally verified under various configurations of the MS-EBG structure. The proposed MS-EBG structure substantially reduces the distance between the noise source and victim devices without degrading the stopband bandwidth. The MS-EBG structure is an alternative power/ground plane for mixed-signal systems in high-density multilayer PCBs.

References

[1] M. Swaminathan et al., "Power Distribution Networks for

System-on-Package: Status and Challenges," *IEEE Trans. Adv. Packag*., vol. 27, no. 2, May 2004, pp. 286–300.

[2] J. Kim et al., "Analysis of Noise Coupling from a Power Distribution Network to Signal Traces in High-Speed Multilayer Printed Circuit Boards," *IEEE Trans. Electromagn. Compat*., vol. 48, no. 2, May 2006, pp. 319–330.

[3] T.-L. Wu et al., "Mitigation of Noise Coupling in Multilayer High-Speed PCB: State of the Art Modeling Methodology and EBG Technology," *IEICE Trans. Commun*., vol. E93.B, no. 7, July 2010, pp. 1678–1689.

[4] T.-L. Wu, H.-H. Chuang, and T.-K. Wang, "Overview of Power Integrity Solutions on Package and PCB: Decoupling and EBG Isolation," *IEEE Trans. Electromagn. Compat*., vol. 52, no. 2, May 2010, pp. 346–356.

[5] E.-P. Li et al., "Progress Review of Electromagnetic Compatibility Analysis Technologies for Packages, Printed Circuit Boards, and Novel Interconnects," *IEEE Trans. Electromagn. Compat*., vol. 52, no. 2, May 2010, pp. 248–265.

[6] R. Abhari and G.V. Eleftheriades, "Metallo-Dielectric Electromagnetic Bandgap Structures for Suppression and Isolation of the Parallel-Plate Noise in High-Speed Circuits," *IEEE Trans. Microw. Theory Techn*., vol. 51, no. 6, June 2003, pp. 1629–1639.

[7] S. Shahparnia and O.M. Ramahi, "Miniaturized Electromagnetic Bandgap Structures for Broadband Switching Noise Suppression in PCBs," *Electron. Lett*., vol. 41, no. 9, Apr. 2005, pp. 519–520.

[8] M. Kwon, M. Kim, and D.G. Kam, "Optimization of a Defected Ground Structure to Improve Electromagnetic Bandgap Performance," *J. Electromagn. Eng. Sci*., vol. 14, no. 4, Dec. 2014, pp. 346–348.

[9] J. Choi et al., "Noise Isolation Inmixed-Signal Systems Using Alternating Impedance Electromagnetic Bandgap (AI-EBG) Structure-Based Power Distribution Network (PDN)," *IEEE Trans. Adv. Packag*., vol. 33, no. 1, Feb. 2010, pp. 2–12.

[10] Y. Toyota et al., "Stopband Analysis Using Dispersion Diagram for Two-Dimensional Electromagnetic Bandgap Structures in Printed Circuit Boards," *IEEE Microw. Wireless Compon. Lett*., vol. 16, no. 12, Dec. 2006, pp. 645–647.

[11] T.-L. Wu, Y.-H. Lin, and S.-T. Chen, "A Novel Power Planes with Low Radiation and Broadband Suppression of Ground Bounce Noise Using Photonic Bandgap Structures," *IEEE Microw. Wireless Comp. Lett*., vol. 14, no. 7, July 2004, pp. 337–339.

[12] M. Kim et al., "Application of VSI-EBG Structure to High-Speed Differential Signals for Wideband Suppression of Common-Mode Noise," *ETRI J*., vol. 35, no. 5, Oct. 2013, pp. 827–837.

[13] M. Kim et al., "Vertical Stepped Impedance EBG (VSI-EBG) Structure for Wideband Suppression of Simultaneous Switching Noise in Multilayer PCBs," *IEEE Trans. Electromagn. Compat*., vol. 55, no. 2, Apr. 2013, pp. 307–314.

[14] H.-R. Zhu and J.-F. Mao, "Localized Planar EBG Structure of CSRR for Ultrawideband SSN Mitigation and Signal Integrity Improvement in Mixed-Signal Systems," *IEEE Trans. Compon., Packag., Manuf. Technol*., vol. 3, no. 12, 2013, pp. 2092–2100.

[15] J.H. Kwon et al., "Novel Electromagnetic Bandgap Array Structure on Power Distribution Network for Suppressing Simultaneous Switching Noise and Minimizing Effects on High Speed Signals," *IEEE Trans. Electromagn. Compat*., vol. 52, no. 2, May 2010, pp. 365–372.

[16] J.H. Kwon and J.G. Yook, "Partial Placement of EBG on Both Power and Ground Planes for Broadband Suppression of Simultaneous Switching Noise," *IEICE Trans. Commun*., vol. E92.B, no. 7, July 2009, pp. 2550–2553.

[17] J.H. Kwon et al., "Partial Placement of Electromagnetic Bandgap Unit Cells to Effectively Mitigate Simultaneous Switching Noise," *Electron. Lett*., vol. 44, no. 22, Oct. 2008, pp. 1302–1303.

[18] C.-L. Wang et al., "A Systematic Design to Suppress Wideband Ground Bounce Noise in High-Speed Circuits by Electromagnetic-Bandgap-Enhanced Split Powers," *IEEE Trans. Microw. Theory Techn*., vol. 54, no. 12, 2006, pp. 4209–4217.

[19] R.E. Collin, *Field Theory of Guided Waves*, New York, USA: IEEE Press, 1991.

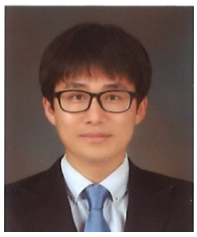

Myunghoi Kim received his BS, MS, and his PhD degrees in electrical engineering at the Korea Advanced Institute of Science and Technology, Daejeon, Rep. of Korea in 2003, 2005, and 2012, respectively. From 2005 to 2008, he was a researcher in the areas of signal integrity and EMC analysis of missile electronic systems at the Agency for Defense Development, Daejeon, Rep. of Korea. He was a visiting researcher at Silicon Image, Inc., Sunnyvale, CA, USA in 2011. From 2012 to 2015, he was a senior member of the engineering staff at ETRI, Daejeon, Rep. of Korea. In 2015, he joined the Department of Electric, Electronic, and Control Engineering at Hankyong National University, Anseong, Rep. of Korea as an assistant professor. His current research interests include signal and power integrity for high-speed packages and PCBs, electromagnetic shielding analysis using a reverberation chamber, and slow-wave/ electromagnetic bandgap structures for EMI/EMC.